

Effect of Albumin and Fibrinogen on Calcium Phosphate Formation on Sol–Gel-Derived Titania Coatings in Vitro

S. Areva,^{*,†,‡} T. Peltola,[§] E. Säilynoja,[‡] K. Laajalehto,^{||} M. Lindén,[†] and J. B. Rosenholm[†]

Department of Physical Chemistry, Åbo Akademi University, Porthansgatan 3-5, FIN-20500 Åbo, Finland, Turku Centre for Biomaterials, Tykistökatu 4D, FIN-20520 Turku, Finland, Institute of Dentistry, University of Turku, Lemminkäisenkatu 2, FIN-20520 Turku, Finland, and Department of Applied Physics, Laboratory of Materials Science, University of Turku, FIN-20014 Turku, Finland

Received August 9, 2001. Revised Manuscript Received January 2, 2002

The sol–gel technique provides a method to produce porous titania (TiO₂) coatings, which are known to induce bone-like hydroxyapatite formation on their surface in vitro. In this study, the calcium phosphate formation (in vitro bioactivity) on a sol–gel-derived titania coating was investigated in vitro in a simulated body fluid in the presence and absence of albumin (BSA) and fibrinogen (Fib) in solution as well as the effect of surface immobilized proteins on the biomineralization process. The effect of proteins on calcium phosphate (CP) formation was followed by ion concentration analysis, XRD, SEM-EDX, and XPS. When BSA and Fib were present in solution, the CP layer growth kinetics were strongly retarded. It is suggested that the bone-like apatite formation on sol–gel-derived titania coatings occurs via continuous dissolution/reprecipitation processes, where the initially formed CP phase(s) recrystallizes into a more thermodynamically stable phase(s), as previously observed for other biomaterials. Inhomogeneous charging was observed in the XPS experiments, which could be used to distinguish between an amorphous CP layer and poorly crystalline CP regions.

Introduction

The formation of a calcium phosphate (CP) layer on the surface of an implant material has wide medical implications in orthopedic, dental, and cardiovascular surgery. Materials such as bioactive glass, sintered hydroxyapatite, and glass-ceramics are known to spontaneously bond to living bone in the body and are clinically widely used bone-repairing materials.¹ The formation of a biologically active CP layer on the implant surface is considered crucial for their integration with bone, and materials having the capability of inducing CP layer formation on their surfaces are often referred to as bioactive materials.^{2,3}

Also titanium and some of its alloys are biocompatible metallic materials coupled with a high strength and fracture toughness, and they have been used, e.g., in orthopedic and dental implants.^{4,5} The use of titanium

as an implant material is based on the good biocompatibility properties of its surface oxide layer, which is generally considered bioinert,⁶ despite reports of direct bonding to bone.^{7,8} Titanium surfaces are known to spontaneously nucleate a CP layer when in contact with simulated body fluids (SBFs) thus improving the biocompatibility properties of the surface and the implant–bone tissue bonding. CP nucleation properties of titanium implants can be enhanced by simple chemical treatments such as soaking in NaOH^{9,10} and H₂O₂^{11,12} solutions with subsequent heat treatments as well as by coating the substrate with a porous sol–gel-derived TiO₂ film.¹ A recent paper by Peltola et al.¹³ emphasized the importance of the titania layers' surface topography in the nanometer scale for the CP formation. The struc-

* To whom correspondence should be addressed. E-mail: sajoar@utu.fi.

[†] Åbo Akademi University.

[‡] Turku Centre for Biomaterials.

[§] Institute of Dentistry, University of Turku.

^{||} Laboratory of Materials Science, University of Turku.

(1) Li, P. Ph.D. Thesis, University of Leiden, Leiden, The Netherlands, 1993.

(2) Martin, R. I.; Brown, P. W. *J. Mater. Sci.: Mater. Med.* **1994**, *5*, 96.

(3) Serro, A. P.; Fernandes, A. C.; Saramago, B.; Lima, J.; Barbosa, M. A. *Biomaterials* **1997**, *18*, 963.

(4) Ellingsen, J. E. *Biomaterials* **1991**, *12*, 593.

(5) Sittig, C.; Hähner, G.; Marti, A.; Textor, M.; Spencer, N. D.; Hauert, R. *J. Mater. Sci.: Mater. Med.* **1999**, *10*, 191.

(6) Hench, L. L. In *Bioceramics* 7; Andersson, Ö. H., Happonen, R.-P., Yli-Urpo, A., Eds.; Butterworth-Heinemann: Oxford, England, 1994; pp 3–14.

(7) Sennerby, L.; Thomsen, P.; Ericson, L. E. *J. Mater. Sci.: Mater. Med.* **1992**, *3*, 262.

(8) Steflif, D. E.; Sisk, A. L.; Parr, G. R.; Gardner, L. K.; Hanes, P. J.; Lake, F. T.; Berkery, D. J.; Brewer, P. *J. Biomed. Mater. Res.* **1993**, *27*, 791.

(9) Kokubo, T.; Kim, H.-M.; Nishiguchi, S.; Nakamura, T. *Key Eng. Mater.* **2000**, 192–195, 3.

(10) Kim, H.-M.; Miyaji, F.; Kokubo, T.; Nishiguchi, S.; Nakamura, T. *J. Biomed. Mater. Res.* **1999**, *45*, 100.

(11) Takemoto, S.; Tsuru, K.; Hayakawa, S.; Osaka, A.; Takashima, S. *Key Eng. Mater.* **2000**, 192–195, 35.

(12) Wang, X.-X.; Hayakawa, S.; Tsuru, K.; Osaka, A. *J. Biomed. Mater. Res.* **2000**, *52*, 171.

(13) Peltola, T.; Jokinen, M.; Rahiala, H.; Pätsi, M.; Heikkilä, J.; Kangasniemi, I.; Yli-Urpo, A. *J. Biomed. Mater. Res.* **2000**, *51*, 200.

ture of the outermost surface can be modified by controlling the sol-aging time and the number of coating layers.

It is generally agreed that the precipitation process from supersaturated CP solutions involves a number of CP phases.^{14–16} At least six of these phases are of biological importance including dicalcium phosphate dihydrate (DCPD, $\text{CaHPO}_4 \cdot 2\text{H}_2\text{O}$), monobasic calcium phosphate (MCP, $\text{Ca}(\text{H}_2\text{PO}_4)_2 \cdot 2\text{H}_2\text{O}$), β -tricalcium phosphate (β -TCP, β - $\text{Ca}_3(\text{PO}_4)_2$), amorphous calcium phosphate (ACP, $\text{Ca}_3(\text{PO}_4)_2 \cdot x\text{H}_2\text{O}$), octacalcium phosphate (OCP, $\text{Ca}_8\text{H}_2(\text{PO}_4)_6 \cdot \text{H}_2\text{O}$), and hydroxyapatite (HA, $\text{Ca}_{10}(\text{PO}_4)_6(\text{OH})_2$).^{17–19} HA has attracted the widest interest due to its close chemical resemblance to the bone-like apatite (carbonated hydroxyapatite), which is the main inorganic component in bone and teeth. Thus simultaneous growth and dissolution as well as transformation reactions ($\text{ACP} \rightarrow \text{DCPD} \rightarrow \text{OCP} \rightarrow \text{HA}$) must be taken into account in any physical–chemical study aimed at simulating such systems.²⁰

The fluid media usually chosen to simulate biological fluids have a similar chemical composition to that of blood but they are free of many biologically important substances, e.g., proteins. However, it has been shown that many of the low and high molecular weight substances in blood have a major influence on the nucleation and growth of the CP precipitate in supersaturated CP solutions.^{2,20–28} These studies reveal that proteins found in mineralized tissues regulate the mineralization process either as nucleators or inhibitors or they have a dual role in the process. Rapid adsorption of plasma proteins has been shown to be one of the first events occurring when blood contacts with foreign material. The protein layer mediates interactions between the surface and cellular components of blood and hence plays a prominent role in the blood and tissue compatibility of biomaterials.²⁹ However, the diversity of the systems used to study HA formation in the presence of proteins makes an overall conclusion difficult to draw and the question remains whether the proteins have the same effect on the CP layer formation on a bioactive surface regardless of the biomaterial used.

(14) Posner, A. S. *Clin. Orthop. Relat. Res.* **1985**, 200, 87.

(15) Nancollas, G. H.; Zieba, A. In *Mineral scale formation and inhibition*; Amjab, Z., Ed.; Plenum Press: New York, 1995; pp 1–9.

(16) van Kemenade, M. J. J. M.; de Bruyn, P. L. *J. Colloid Interface Sci.* **1987**, 118, 564.

(17) Lu, H. B.; Campbell, C. T.; Graham, D. J.; Ratner, B. D. *Anal. Chem.* **2000**, 72, 2886.

(18) Chusuei, C. C.; Goodman, W.; van Stipdonk, M. J.; Justes, D. R.; Schweikert, E. A. *Anal. Chem.* **1999**, 71, 149.

(19) Chusuei, C. C.; Goodman, D. W.; van Stipdonk, M. J.; Justes, D. R.; Loh, K. H.; Schweikert, E. A. *Langmuir* **1999**, 15, 7355.

(20) Johnsson, M. S.-A.; Pashalis, E.; Nancollas, G. H. In *The Bone-Biomaterial Interface*; Davies, J. E., Ed.; University of Toronto Press: Toronto, 1991; pp 68–75.

(21) Koutsopoulos, S.; Dalas, E. *Langmuir* **2000**, 16, 6739.

(22) Romberg, R. W.; Werness, P. G.; Riggs, B. L.; Mann, K. G. *Biochemistry* **1986**, 25, 1176.

(23) Hunter, G. K.; Kyle, C. L.; Goldberg, H. A. *Biochem. J.* **1994**, 300, 723.

(24) Hunter, G. K.; Hauschka, P. V.; Poole, A. R.; Rosenberg, L. C.; Goldberg, H. A. *Biochem. J.* **1996**, 314, 59.

(25) Daculsi, G.; Pilet, P.; Cottrel, M.; Guicheux, G. *J. Biomed. Mater. Res.* **1999**, 47, 228.

(26) Tsortos, A.; Ohki, S.; Zieba, A.; Baier, R. E.; Nancollas, G. H. *J. Colloid Interface Sci.* **1996**, 177, 257.

(27) Ebrahimpour, A.; Perez, L.; Nancollas, G. H. *Langmuir* **1991**, 7, 577.

(28) Misra, D. N. *J. Colloid Interface Sci.* **1997**, 194, 249.

(29) Slack, S. M.; Horbett, T. A. *J. Colloid Interface Sci.* **1988**, 124, 535.

In the present work, sol–gel-derived titania coatings with controlled surface topography were immersed in SBF with or without the bovine serum albumin (BSA) and bovine fibrinogen (Fib). Albumin was chosen as a model protein, because it is the most abundant protein in blood plasma, and fibrinogen was chosen for its importance in cell attachment and the previously observed dual role in CP formation. The influence of proteins on CP formation was followed with calcium and phosphate ion concentration variations in the SBF solution by ion concentration analysis. The structure, composition, and morphology of the formed CP layer was analyzed with scanning electron microscopy coupled with energy-dispersive X-ray (SEM-EDX), X-ray diffraction (XRD) analysis, and X-ray photoelectron spectroscopy (XPS).

Materials and Methods

Substrate Preparation. Commercially pure (c.p.) titanium was used as a substrate material for the experiments. Titanium was ground by silicon carbide papers having 500, 800, and 1200 grits and washed ultrasonically in acetone and ethanol for 5 + 5 min before dipping into the sol. The titania coatings on the titanium substrate were prepared by the sol–gel dip-coating technique as described by Jokinen et al.³⁰ Briefly, the sol was prepared by dissolving tetraisopropylorthotitanate [$\text{Ti}(\text{OCH}(\text{CH}_3)_2)_4$] into absolute ethanol (solution I). Solution II was prepared by mixing ethyleneglycolmonoethyl ether ($\text{C}_2\text{H}_5\text{OCH}_2\text{CH}_2\text{OH}$), deionized water, and 1 M hydrochloric acid (37%) with absolute ethanol. Solutions I and II were mixed at room temperature with vigorous stirring. The clear sol was kept at 0 °C during aging and the dip-coating process. The coating procedure started after 24 h of sol-aging, and the number of coating layers was 5. After deposition of each layer, the substrates were sintered at 500 °C for 10 min, subsequently cleaned in an ultrasonic bath with acetone and ethanol (5 + 5 min), and finally dried in air. Coated titanium disks were cut into pieces having dimensions of 1 × 1 cm².

Simulated Body Fluid (SBF) Tests. The in vitro bioactivity of the samples and the influence of proteins was studied using a so-called Kokubo's³¹ SBF. Briefly, SBF was prepared by dissolving reagent chemicals of NaCl, NaHCO_3 , KCl, $\text{K}_2\text{HPO}_4 \cdot 3\text{H}_2\text{O}$, $\text{MgCl}_2 \cdot 6\text{H}_2\text{O}$, CaCl_2 , and Na_2SO_4 into deionized water. The fluid was buffered at physiologic pH 7.40 at 37 °C with the tris-buffer reagents [$(\text{CH}_2\text{OH})_3\text{CNH}_2$ and $(\text{CH}_2\text{OH})_3\text{CNH}_2 \cdot \text{HCl}$] and 1 M hydrochloric acid. The ion concentrations of SBF (Na^+ , 142.0; K^+ , 5.0; Mg^{2+} , 1.5; Ca^{2+} , 2.5; Cl^- , 147.8; HCO_3^- , 4.2; HPO_4^{2-} , 1.0; SO_4^{2-} , 0.5 mM) are nearly equal to that of human plasma.³² All of the SBF reagents were obtained from Merck except the tris-buffer reagents, which were from Sigma. BSA (A 4503, fraction V) as well as Fib (F-8630; fraction I), which contains 76% fibrinogen, 10% sodium citrate, and approximately 15% NaCl, were purchased from Sigma. The proteins were used without further purification. Protein solutions were prepared by weighing and dissolving 1 mg/mL of BSA and 0.1 mg/mL of Fib into SBF. The protein concentrations were determined using a Micro BCA Protein Assay Reagent Kit before immersion. The measured BSA and Fib concentrations were 1.00 ± 0.03 and 0.083 ± 0.002 mg/mL, respectively. All solutions were filtered through a 0.45 μm filter before use.

Titanium substrates coated with titania layers were immersed in 22 mL of SBF, SBF + BSA, and SBF + Fib solutions to give a surface area to solution volume (SA/V) ratio of 0.1.

(30) Jokinen, M.; Pätsi, M.; Rahiala, H.; Peltola, T.; Ritala, M.; Rosenholm, J. B. *J. Biomed. Mater. Res.* **1998**, 42, 295.

(31) Kokubo, T.; Kushitani, H.; Sakka, S.; Kitsugi, T.; Yamamuro, T. *J. Biomed. Mater. Res.* **1990**, 28, 721.

(32) Cho, S.-B.; Kokubo, T.; Kitsugi, T.; Nakamura, T.; Nakanishi, K.; Ohtsuki, C.; Soga, N.; Yamamuro, T. *J. Am. Ceram. Soc.* **1995**, 78, 1769.

Solutions were kept in a polyethylene bottle covered with a tight lid and placed in a shaking water bath at 37 °C for 2–14 days. Some of the samples were pretreated with tris-buffered sodium chloride (150 mM) solutions at 37 °C for 15 h containing BSA (1 mg/mL; preBSA) and Fib (0.1 mg/mL; preFib). Pretreated samples were gently washed with deionized water (to remove any loosely adsorbed proteins), dried, and immersed in SBF for 14 days as mentioned earlier. SBF, SBF + BSA, and SBF + Fib solutions without the titania samples were used as a control. Triplicate samples were used for all solution conditions. The experiments were performed under sterile conditions in a laminar flow cabinet to avoid bacterial growth in the tubes. After immersion, samples were taken from the fluids, rinsed with deionized water, dried in laminar flow cabinet, and stored in a vacuum desiccator before surface analysis.

Ion Concentration Analysis. Sample solutions were monitored for calcium and phosphate as a function of immersion time. Calcium concentrations were determined by atomic adsorption spectrophotometer (Perkin-Elmer 460). Phosphate concentrations were analyzed spectrophotometrically (Shimadzu UV-1601) by the molybdenum blue method. Triplicate samples were analyzed.

Surface Analysis. The surface topography and roughness of the titania film before immersion was determined by the noncontact tapping mode atomic force microscopy (AFM) using a NanoScope III multimode AFM (Digital Instruments, Santa Barbara, CA) apparatus. The XRD patterns of titania surfaces immersed in SBF, SBF + BSA, and SBF + Fib solutions were collected with a Phillips "X'pert" PW-3020 X-ray diffractometer. The XRD patterns were measured in the 2θ region between 20 and 50° with the step size of 0.02° and a scan time of 2s/step. Cu K α_1 radiation ($\lambda = 1.54056 \text{ \AA}$) was used with the X-ray tube voltage of 40 kV and the current of 30 mA.

Morphology and chemical analysis of the samples were performed using a scanning electron microscope equipped with an energy-dispersive X-ray analyzer (SEM-EDX, Stereoscan 360 Cambridge). Further information of the chemical nature of the outermost part of the films was obtained by X-ray photoelectron spectroscopy (XPS, Perkin-Elmer PHI 5400 ESCA System Spectrometer). The XPS measurements were performed at a base pressure of 1×10^{-8} Torr using the Mg K α X-ray ($\lambda = 1253.6 \text{ eV}$) source. The electron analyzer pass energy in the XPS high-resolution scans was 35.75 eV. The grazing angle of the photoelectrons was 45° if not otherwise stated. The UNIFITTU (version 2.1) software was used for peak fitting and quantitative chemical analysis, applying sensitivity factors given by the manufacturer of the instrument. The high-resolution spectra were charge compensated by setting the binding energy (BE) of the C 1s contamination peak to 284.6 eV.³³

Results

Concentration Analysis. Since calcium (Ca^{2+}) and phosphate ($\text{HPO}_4^{2-}/\text{PO}_4^{3-}$) are required for the CP generation, the reduction of their concentrations in SBF indicates the formation of CP on the titania coatings. The Ca^{2+} concentration evolution in SBF solution as a function of time is presented in Figure 1 and $\text{HPO}_4^{2-}/\text{PO}_4^{3-}$ in Figure 2. CP nucleation was apparent after 2 days of immersion while fast growth of the CP layer occurred after 5 days of immersion. When BSA (SBF + BSA) and Fib (SBF + Fib) were present in the solution, the consumption of Ca^{2+} and PO_4^{3-} was greatly decreased when compared to the samples immersed in pure SBF. There was, however, a slight decrease in both the Ca^{2+} and PO_4^{3-} concentrations indicating that the

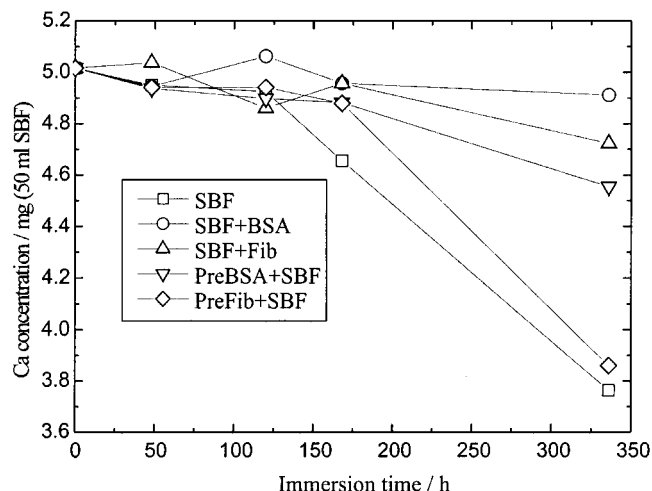


Figure 1. Evolution of calcium concentration in SBF as a function of substrate immersion time.

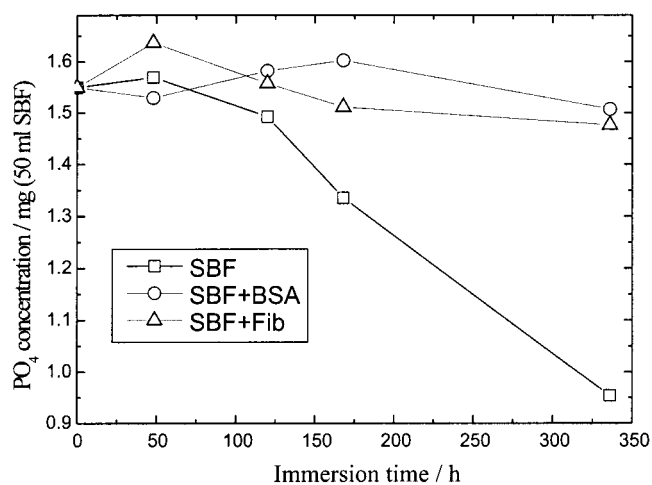


Figure 2. Evolution of phosphate concentration in SBF as a function of substrate immersion time.

CP nucleation was not totally prevented in the presence of BSA and Fib.

When the coatings were pretreated with the BSA (preBSA) and Fib (preFib) solutions before immersion in SBF, there were notable differences in the behavior of the two proteins regarding the CP formation. For the BSA pretreated samples, the decrease in both Ca^{2+} and PO_4^{3-} concentrations after 14 days of immersion was enhanced compared to the situation where BSA was present in solution. Thus, when BSA was adsorbed on the surface before immersion in SBF it slowed the CP formation but the inhibition effect was not as strong as when BSA was present in solution. In the case of Fib pretreated samples, the ion concentration decrease was similar to that of the untreated samples in SBF. It should be noted that the error margins in the pretreated samples were significantly larger than for the other samples, which could indicate that the adsorbed protein layers were not continuous. The Ca/P ratios calculated based on ion concentration data were generally close to the theoretical values of HA (1.67), except the Ca/P value (1.42) for the samples pretreated with BSA which were closer to the theoretical value of ACP (1.50) and OCP (1.33) (Table 1).

Surface Analysis. AFM measurements were routinely performed to check the topography of the titania

(33) Mullenberg, G. E. *Handbook of X-ray photoelectron spectroscopy*; Perkin-Elmer Corporation: Eden Prairie, MN, 1979.

Table 1. Calculated Ca/P Ratios Based on Solution, SEM-EDX, and XPS Analyses after 14 Days of Immersion

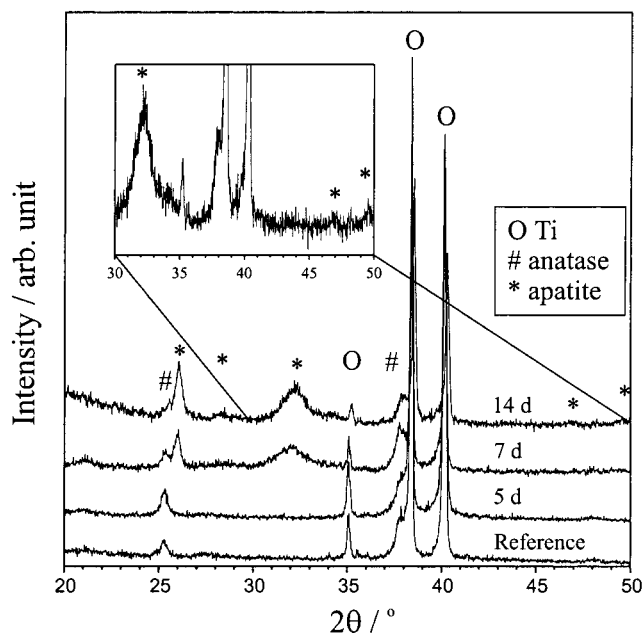
| immersion conditions | Ca/P ratio | | |
|----------------------|--------------------|------|------|
| | ion concn analysis | EDX | XPS |
| SBF | 1.62 | 1.71 | 1.27 |
| SFB + BSA | | | 0.83 |
| SFB + Fib | | | 1.07 |
| preBSA + SBF | 1.42 | 1.51 | 1.14 |
| preFib + SBF | 1.66 | 1.59 | 1.28 |

films before immersion in SBF. The data (not shown) were compared to the previously reported surface structure of the films.³⁰ The optimum nanostructure of the films were reproducibly obtained.

Further information on the structure of the titania film and the CP layer was obtained by the XRD measurements. The most intensive reflections observed originated from the [100], [002], and [101] reflections of the Ti-metal substrate at 35.1, 38.4, and 40.1° (in 2θ), respectively, (Figure 3). Furthermore, the [101] reflection at 25.3° and the reflections [103], [004], and [112] at 37.0–38.0° of anatase were clearly observed, indicating that some of the sol-gel-derived titania coating had transformed into anatase during the heat treatment, while the rest remained amorphous. The patterns obtained as a function of immersion time offered reliable proof that the partly amorphous calcium phosphate layer has the same features as bone-like apatite¹⁴ after 7 days of immersion in SBF. Broad reflections at 30.7–34.5° (in 2θ) resulting from the [211], [112], and [300] reflections of HA³⁴ indicate poor crystallinity of the formed HA. In the presence of proteins, no reflections resulting from the CP phases were detected even after 14 days of immersion. However, the XRD patterns of the BSA and Fib pretreated samples immersed for 14 days in SBF showed the presence of bone-like apatite (not shown). No other CP phases could be detected in any of the samples.

SEM photographs of the titania surfaces immersed in SBF solutions for 14 days verified the observations from the ion concentration and the XRD analysis. CP layer was detected in the sample immersed in pure SBF and in the protein pretreated samples. The most developed CP layer was observed on the coatings immersed in pure SBF (Figure 4a). The BSA pretreated coatings exhibited less CP than the Fib pretreated coatings. In SBF + BSA and SBF + Fib conditions, the presence of a CP layer was not detected even after 14 days of immersion. From the SEM images, it can be seen that on the BSA and Fib pretreated surfaces (Figures 4b and 4c) the formed CP is more evenly distributed than in the absence of proteins (Figure 4a). The Ca/P ratios obtained from the EDX analysis (Table 1) closely resembled those calculated based on the ion concentration analysis.

XPS analysis was used to determine the elemental composition of the outermost portion of the surface layer after immersion in the SBF solutions for various time periods (Tables 2 and 3). Calcium (Ca $2p_{3/2}$) and phosphorus (P $2p_{3/2}$) peaks were detected at the first sample retrieval point (2 days) having binding energies (BEs) of ~347.1 and ~133.0 eV, respectively, in the

**Figure 3.** XRD patterns of titania coatings immersed in SBF as a function of time.**Table 2. Relative Atomic Percentages (Obtained By XPS) as a Function of Immersion Time in SBF**

| immersion conditions | immersion time (days) | C | O | Ti | Ca | P | N | Ca/Ti |
|-----------------------|-----------------------|------|------|------|------|------|------|-------|
| ref. TiO ₂ | | 30.6 | 50.7 | 18.7 | | | | |
| SBF | 14 | 16.4 | 55.2 | 4.4 | 13.5 | 10.6 | | 3.04 |
| SBF | 7 | 14.8 | 58.0 | 6.7 | 10.6 | 8.8 | | 1.59 |
| SBF | 5 | 24.1 | 55.4 | 15.6 | 2.2 | 2.1 | 0.6 | 0.14 |
| SBF | 2 | 33.5 | 48.4 | 15.2 | 1.4 | 1.5 | | 0.09 |
| SFB + BSA | 14 | 49.2 | 31.0 | 4.9 | 1.0 | 1.2 | 12.7 | 0.21 |
| SFB + BSA | 2 | 46.4 | 35.3 | 8.4 | 1.1 | 1.2 | 7.7 | 0.13 |
| SFB + Fib | 14 | 53.5 | 27.0 | 4.0 | 0.8 | 0.8 | 14.0 | 0.20 |
| SFB + Fib | 2 | 56.4 | 25.8 | 3.0 | 0.5 | 0.5 | 13.9 | 0.16 |
| preBSA + SBF | 14 | 33.8 | 44.9 | 10.0 | 3.0 | 2.7 | 5.7 | 0.30 |
| preFib + SBF | 14 | 36.1 | 39.5 | 5.0 | 6.0 | 4.6 | 8.7 | 1.19 |

presence and absence of proteins. In the presence of proteins, the Ca concentration increased slightly as seen from the Ca/Ti values but the BEs did not change even after 14 days of immersion. Since nitrogen was not detected in the reference sample, the presence of the N 1s peak is indicative of protein on the surface.

After 7 days of immersion in pure SBF, however, two Ca (BEs = ~347.2 and ~350.4 eV) and P (BEs = ~133.0 and ~136.1 eV) peaks were detected. At the same time, the BE of the Ti $2p_{3/2}$ peak remained constant (~458.5 eV), and from the fact that another impurity carbon peak appeared with the same binding energy shift as that of Ca and P, it could be concluded that this shift resulted from inhomogeneous charging of the surface (Table 3 and Figure 5). The relative areas of the charge-shifted peaks increased and the area of the nonshifted peaks decreased as the CP layer grew but the charge shift did not increase as a function of either CP layer growth or measuring time.

To further study the CP layer detected by XPS, the Ca/P ratios were calculated. In Table 1, the Ca/P ratios calculated from the total Ca and P peak areas are shown. When these results are compared to the ion concentration analysis results, it can be seen that Ca/P ratios increase as more Ca²⁺ and HPO₄²⁻/PO₄³⁻ ions are consumed from the solution. The outer layer of the

(34) Li, P.; de Groot, K.; Kokubo, T. *J. Am. Ceram. Soc.* **1994**, *77*, 1307.

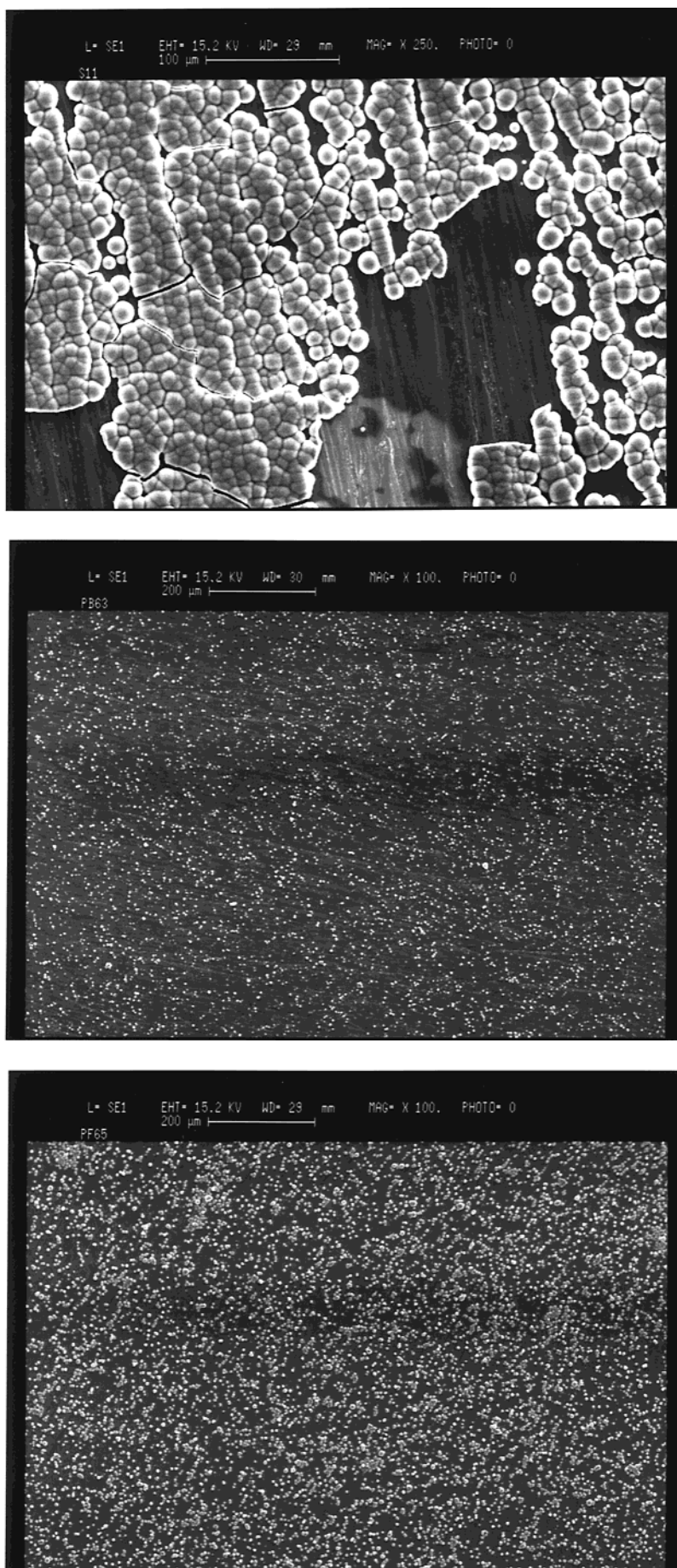


Figure 4. SEM photographs of the coating after 14 days of immersion in SBF: without pretreatment (a), pretreated with BSA (b), and pretreated with Fib (c).

Table 3. Binding Energies (eV) of the Components Calculated from the High Resolution XPS Data; Percentage (%) of the Individual Component Is Shown in Brackets and the Ca/P Ratios Are Calculated for the Ca and P Peaks Appearing at Different Binding Energies; Sample SBF 14d Marked with # Is Measured Using a Grazing Angle of 0°

| immersion conditions | C 1s | Ti 2p _{3/2} | Ca 2p _{3/2} | P 2p _{3/2} | Ca/P |
|-------------------------|--|----------------------|------------------------------|------------------------------|--------------|
| ref. TiO ₂ | 284.6 (71.0) 285.9 (19.4) 288.3 (9.6) | 458.5 (100) | | | |
| SBF 14 days | 284.6 (18.4) 288.0 (75.3) 292.5 (6.3) | 458.5 (100) | 347.6 (3.5) 350.5 (96.5) | 133.0 (4.5) 136.4 (95.5) | 0.98 1.29 |
| SBF # 14 days | 284.6 (85.0) 286.3 (6.0) 288.1 (9.0) | 458.2 (100) | 347.1 (53.4) 350.7 (46.6) | 133.0 (64.6) 136.7 (35.4) | 0.92 1.48 |
| SBF 7 days | 284.6 (24.4) 285.9 (11.5) 288.0 (51.0) 289.7 (6.4) 291.9 (6.7) | 458.5 (100) | 347.3 (6.8) 350.3 (93.2) | 133.0 (9.7) 136.1 (90.3) | 0.84 1.24 |
| SBF 5 days | 284.6 (62.1) 286.0 (24.7) 288.3 (13.2) | 458.4 (100) | 347.1 (100) | 132.7 (100) | 1.07 |
| SBF + BSA 14 days | 284.6 (46.6) 285.9 (30.9) 287.9 (22.5) | 458.3 (100) | 347.0 (100) | 132.6 (100) | 0.85 |
| SBF + Fib 14 days | 284.6 (48.4) 285.9 (27.7) 287.8 (24.0) | 458.2 (100) | 346.9 (100) | 132.5 (100) | 1.06 |
| preBSA + SBF 14 days | 284.6 (50.5) 286.0 (26.2) 288.0 (23.3) | 458.3 (100) | 347.0 (56.5) 350.7 (43.5) | 132.7 (58.8) 136.2 (41.2) | 1.09 1.20 |
| preFib + SBF 14 days | 284.6 (42.6) 285.9 (29.3) 288.0 (28.0) | 458.3 (100) | 346.9 (12.0) 350.9 (88.0) | 132.4 (15.1) 136.5 (84.9) | 1.03 1.33 |

titania coating immersed for 14 days in pure SBF was also measured at 0° grazing angle for increased surface sensitivity. The peak splitting of the Ca peak is more pronounced, and the two components are easily detected (Figure 6). The same phenomenon was observed in the high-resolution spectrum of phosphorus. The calculated Ca/P ratios for 45 and 0° grazing angle measurements were 1.27 and 1.13, respectively. The calculated Ca/P ratios for the charged and uncharged species, respectively, are summarized in Table 3. There is an obvious trend in that the Ca/P ratio of the uncharged peaks is lower (near 1) than for the charged peaks (near 1.3).

Discussion

The effect of proteins on CP formation has been previously studied, for example, for bioglass, ceramics, and titanium. In the presence of proteins, the surface reactions of bioactive glass are slowed and thus alter the elemental depth profile of the surface.^{35,36} Generally, the presence of proteins seem to inhibit the growth and crystallization but not the nucleation of CP.^{37,38} Radin and Ducheyne³⁹ showed that serum proteins did not affect the surface reactions of ceramics similar to bone mineral leading to the formation of carbonated apatite.

However, the surface reactions of the nonapatitic ceramics (e.g., β -TCP and calcium carbonate) used in their study were blocked in the presence of proteins. Studies on titanium surfaces showed that in the presence of proteins, the CP growth was strongly inhibited, although the deposition of Ca²⁺ and PO₄³⁻ occurred.^{3,40,41} The transformation of most synthetic ceramics into bone-like apatite is suggested to occur through dissolution of initial CP phases and reprecipitation of new CP phases and it is suggested that serum proteins inhibit the CP transformation process if it occurs via the dissolution/reprecipitation mechanism.³⁹ These results are well in line with the results obtained in our study. During the two weeks of immersion in SBF in the presence of proteins, Ca²⁺ and PO₄³⁻ consumption from the solution was negligible. Calcium and phosphorus on the titania surface were detectable only by XPS. The retardation effect of preadsorbed protein on the CP growth rate was not as strong as when there was protein present in solution but was still evident in comparison to the standard SBF solution. However, as seen in the SEM images shown in parts a–c of Figure 4, the number of aggregates is higher while the aggregate size is smaller if protein is preadsorbed to the titania surface. This again supports the idea that the presence of proteins does not totally prevent the nucleation of CP but strongly lowers the CP growth rate by lowering the dissolution/reprecipitation rate of CP. Thus, the apatite

(35) Mei, J.; Shelton, R. M.; Marquis, P. M. *J. Mater. Sci.: Mater. Med.* **1995**, *6*, 703.

(36) Effaf Kaufmann, E. A. B.; Ducheyne, P.; Radin, S.; Bonnell, D. A.; Conposto, R. *J. Biomed. Mater. Res.* **2000**, *52*, 825.

(37) Radin, S.; Ducheyne, P.; Rothman, B.; Conti, A. *J. Biomed. Mater. Res.* **1997**, *37*, 363.

(38) Lu, H. H.; Pollack, S. R.; Ducheyne, P. *J. Biomed. Mater. Res.* **2001**, *54*, 454.

(39) Radin, S.; Ducheyne, P. *J. Biomed. Mater. Res.* **1996**, *30*, 273.

(40) do Serro, A. P. V. A.; Fernandes, A. C.; de Jesus, B.; Saramago, V. *Colloid Surf., B* **1997**, *10*, 95.

(41) do Serro, A. P. V. A.; Fernandes, A. C.; de Jesus, B.; Saramago, V. *J. Biomed. Mater. Res.* **2000**, *49*, 345.

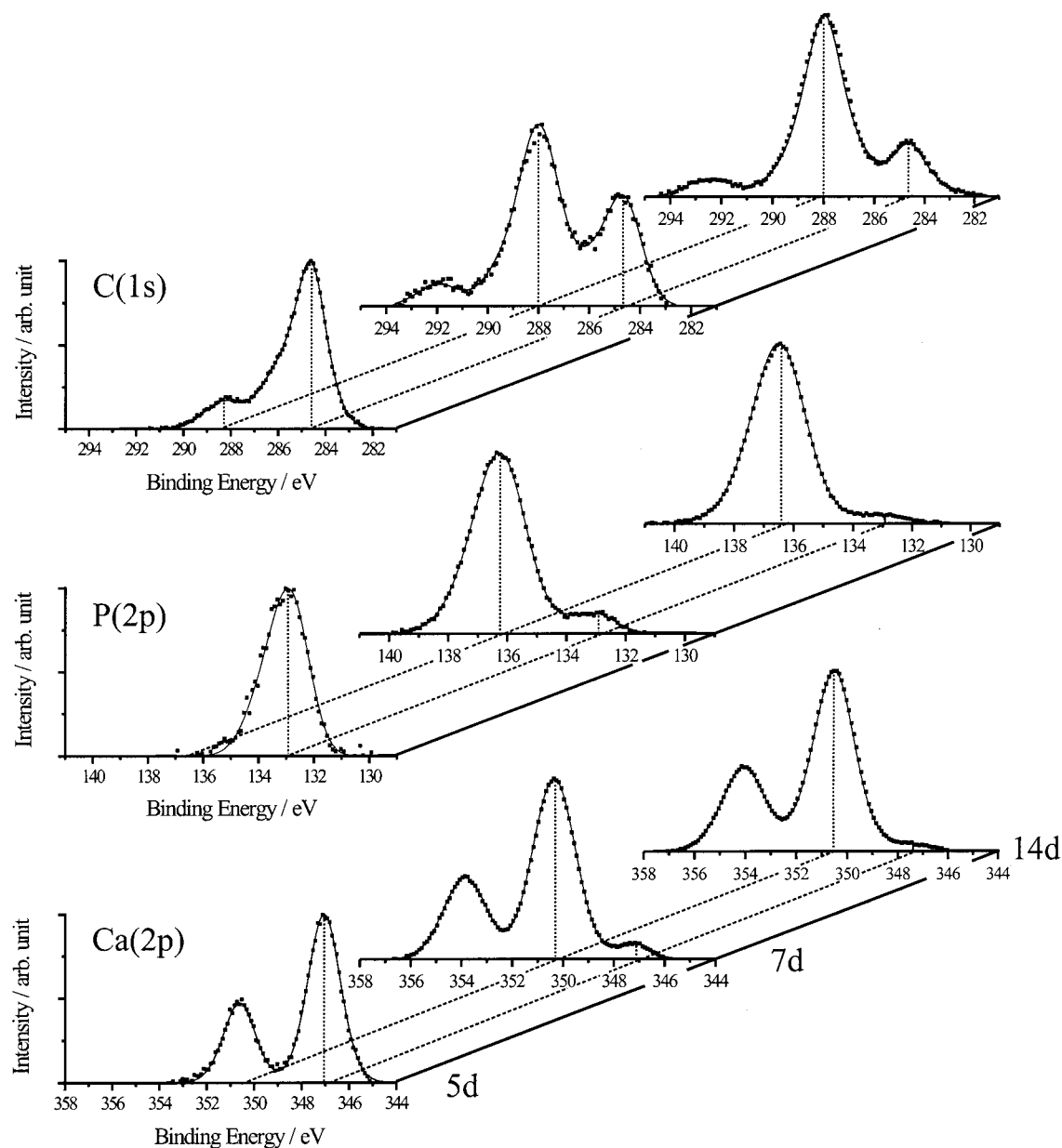


Figure 5. Evolution of calcium, phosphorus, and carbon high-resolution XPS spectra as a function of immersion time in SBF. Dotted lines represent the binding energies of the main components obtained from peak fitting.

formation on sol-gel-derived titania coating occurs via continuous dissolution/precipitation processes. Similar results were reported by Vallet Regi et al.⁴² for bioactive gel glasses where the chemical composition of the CP layer was very heterogeneous consisting of a composition gradient across the layer.

Furthermore, it is suggested that the major influence of the proteins on the CP growth rate is the adsorption to amorphous CP inhibiting the dissolution/precipitation of CP. When present in solution, the proteins had an equally strong inhibitory effect on the CP formation. BSA⁴³ and Fib⁴⁴ have a net negative charge of -9 and -10 , respectively, at physiological conditions, and they may therefore strongly adsorb to Ca-sites of the nucle-

ated CP. Also, the nucleation process was delayed, but the preadsorbed BSA had a stronger inhibiting effect than the preadsorbed Fib. This difference might arise from their different adsorption mechanisms to TiO_2 . While BSA is adsorbed to the TiO_2 surface through Ca^{2+} , Fib has been suggested to adsorb through electrostatic interactions between negatively charged surface hydroxyl groups on the TiO_2 and the positively charged subdomains of the protein.^{43,44} Naturally, any conformational changes of the proteins upon adsorption to the titania surface may play a role for the nucleation and growth of CP, but the rough titania surface makes a quantification of such effects virtually impossible.

In two recent papers, XPS was used to study different CP phases. Chusuei et al.¹⁸ reported that the BEs of Ca $2p_{3/2}$ and P $2p$ differed by only 0.3 and 0.6 eV, respectively, between different CP phases. The calculated Ca/P ratios were 1.59, 1.13, 1.20, and 0.74 for HA, ACP, OCP, and DCPD, respectively, which were some-

(42) Vallet-Regi, M.; Perez-Pariente, J.; Izquierdo-Barba, I.; Salinas, A. J. *Chem. Mater.* **2000**, *12*, 3770.

(43) Klinger, A.; Steinberg, D.; Kohavi, D.; Sela, M. N. *J. Biomed. Mater. Res.* **1997**, *36*, 387.

(44) Yongli, C.; Xiufang, Z.; Yandao, G.; Nanming, Z.; Tingying, Z.; Xinqi, S. *J. Colloid Interface Sci.* **1999**, *214*, 38.

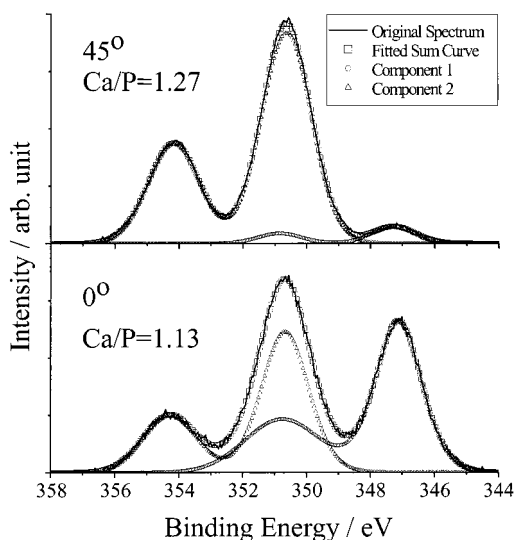


Figure 6. High-resolution XPS spectra of calcium obtained using grazing angles of 45 and 0°.

what smaller than the theoretical values. Furthermore, Lu et al.¹⁷ suggested that the CP phases could be determined by the relationship between the intensities of an O 1s shake-up satellite with the phosphate oxygen content. Due to the complicated peak overlapping of oxygens from phosphate, titania, and protein species, this method could not be used in this study. In this work, we use the observed inhomogeneous surface charging to distinguish between amorphous and poorly crystalline CP. Inhomogeneous charging is usually observed when the insulating overlayer on conductive substrate becomes too thick (approximately 10 nm or more) resulting in distorted peak shapes.⁴⁵ Since no electrical isolation was used in our XPS measurements, inhomogeneous charging was detected as the CP layer grew. The sample charging was observed for the samples for which bone-like apatite was detected by XRD and SEM-EDX. Therefore, we suggest that the inhomoge-

(45) Ratner, B.; Castner, D. In *Surface analysis - The principal techniques*; Vickerman, J. C., Ed.; Wiley: Chichester, England, 1999; pp 43–98.

neous charging separated the calcium and phosphorus peaks resulting from the initially formed amorphous CP phase from the bone-like apatite phase. This conclusion is supported by the Ca/P ratios obtained for the uncharged and charged species, close to 1 and 1.3, respectively, as well as the angle dependence of the relative ratios of the two phases. The thickness of the outer layer is on the order of some nanometers. The Ca/P ratio of about 1.3 observed for the poorly crystalline CP is close to that of OCP, which is why it would be tempting to ascribe the observation to a poorly crystalline intermediate OCP layer. However, small errors in the used sensitivity factors, for example, could account for this difference, and hence we only conclude that we are able to distinguish between an amorphous layer and partly crystalline regions of different composition. However, the bulk of the aggregates clearly consists of carbonated hydroxyapatite as evidenced by the Ca/P ratios obtained from both solutions and EDX as well as the crystallinity observed in the XRD.

Conclusions

Our results suggest that the presence of both albumin and fibrinogen in the SBF delays the growth of CP on the surface of titania coating through decreasing the recrystallization rate of the initially formed amorphous calcium phosphate. The amorphous surface layer has a thickness of some nanometers and is clearly distinguishable from the poorly crystalline portion of the CP layer in the XPS. A preadsorbed protein layer does not delay the recrystallization of CP to the same extent as when the proteins are present in solution. Therefore, it is suggested that the proteins mainly influence the CP nucleation and growth kinetics by adsorbing to the initially formed CP.

Acknowledgment. S.A. thanks Graduate School of Materials Science, Turku, Finland, for financial support. Dr. Kaj Fröberg from the Department of Inorganic Chemistry at Åbo Akademi University is acknowledged for performing the XRD measurements.

CM0107272